

A Library of Training Images for Fluvial and Deepwater Reservoirs and Associated Code

Michael J. Pyrcz (mpyrcz@ualberta.ca) and Clayton V. Deutsch (cdeutsch@ualberta.ca)
Department of Civil & Environmental Engineering
University of Alberta

Geostatistical algorithms that consider multiple-point statistics are becoming increasingly popular. These methods allow for the reproduction of complicated features beyond the commonly implemented two-point statistic: the covariance or semivariogram. In practice, it is not possible to infer many multiple-point statistics directly from the available data; therefore, it is common to borrow statistics from training images. Training images are exhaustive gridded numerical models that have spatial features deemed relevant to the site being characterized.

A library of training images is developed for fluvial and deepwater depositional settings. These training images are based on marked point processes, fluvial and deepwater models. The marked point process models are based on stochastically placed ellipsoids, bars and lobes. The fluvial training images are based on the object based FLUVSIM algorithm and the bank retreat model. The deepwater training images are based on a surface based model of compensational cycles of flow events within turbidite lobes. The training images represent a range of net-to-gross fractions and an assortment a depositional styles.

The associated code includes FORTRAN routines required to modify, format and tailor the training images and to extract multiple-point statistics. This code allows the practitioner to match site specific features and to utilize this library in a variety of applications.

There is a wide range of anticipated applications for this training image library beyond a source for multiple-point statistics. This library may be utilized in comparative flow studies, as type-models for demonstration and training and to aid in scenario based uncertainty studies.

Introduction

Conventional geostatistics is limited to two-point statistics. These techniques are unable to reproduce complicated geometries that are often present in reservoir geology. The omission of these features may result in numerical reservoir models that misrepresent the reservoir response qualified by flow simulation. This limitation has motivated research in geostatistical methods that integrate multiple-point statistics beyond the semivariogram.

The development of geostatistical algorithms that account for multiple-point statistics is not new. These techniques were pioneered by Journel and Alabert (1989) and applied in

simulated annealing by Deutsch (1992). Strebelle (2002) provides a review of the evolution of these multiple-point geostatistical algorithms and a proposed efficient noniterative algorithm (SNESIM).

While these techniques are able to reproduce complicated geometries, characterization of the required multiple-point statistics is often an impossible inference problem. The number of categorical probabilities that must be inferred is K^N for a multiple-point histogram (where K is the number of categories and N is the number of points considered). Note that multiple-point geostatistics is typically restricted to categorical random variables. The a priori requirement of consistent or positive definite multiple-point statistics is satisfied by borrowing these statistics from exhaustively gridded categorical training images.

Training images contain geologic information on the geometries and interrelationships between geologic categories at the required scale. These categories may represent lithofacies or truncated continuous petrophysical properties. Training images may be constructed in a variety of ways, including outcrop mapping, conceptual models from professional geologic judgment and stochastic algorithms. In the latter case the most efficient approach may be to apply of the stochastic algorithm in a conditional mode instead of conditioning by multiple-point methods.

The training image library and associated code described below provide the required multiple-point statistical input that cannot be directly calculated from the data available. These borrowed statistics may be applied in traditional semivariogram based and multiple-point geostatistical algorithms. The associated code may be applied to tailor the training images to a specific site and to format and extract the required multiple-point statistics.

The Training Images

The library includes training images from (1) marked point processes, (2) FLUVSIM (Deutsch and Wang, 1996; Deutsch and Tran, 2002) models, (3) surface based models and (4) bank retreat fluvial models. Model parameters have been set to represent a variety of potential features. For example, each model is generated with a net-to-gross of 0.2, 0.4, 0.6, and 0.8 and channelized models include narrow, median and wide channels. Model parameters are discussed, but details of the algorithms are left in the original references.

The training image scale was selected to be representative of nominal reservoir scale. The models represent a volume of about 4,000m x 4,000m x 20m. It is anticipated that these models are relevant over a wide range of scales from 10% to 1,000% of this volume depending on the level of scale invariance in the specific depositional setting.

The model resolution was chosen as a balance between adequately characterizing the simulated features for export of multiple-point statistics and portability, computation and storage requirements. Additionally, the rapid increase in available computational power

was considered. The models are discretized by 256x256x128 with resulting 8.6 million cells (see Figure 1). A summary of the models in the training image library is provided in Table 1. A total of 498 training images are provided.

Marked Point Training Images

These training images are based on concepts from stochastic geometry (Stoyan et al, 1987). A Poisson point process with or without stationary intensity may be applied to position germs. Primary grains, or parameterized objects, are then positioned relative to the germs.

The marked point training images are binary models with stationary intensity of germs and a variety of primary grains representing ellipsoids, bars and lobes. Geometric templates characterize the primary grains (the associated geometries are shown in Figure 2). The germ locations are drawn from a uniform distribution of the training image space. The associated orientation and scale are drawn from triangular distributions (illustrated in Figure 3).

- Azimuth $0^\circ \pm 30^\circ$
- Dip $0^\circ \pm 3^\circ$
- Plunge $0^\circ \pm 5^\circ$
- Scale $\pm 20\%$

Primary grains are stochastically added until the net-to-gross ratio is met. The results are smoothed by the maximum a-posteriori selection (MAPS) (Deutsch, 1998a) method to remove any discretization artifacts.

FLUVSIM Training Images

Interest in North Sea fluvial reservoirs led to the development of object based models for fluvial facies and geometries (Clemensten et al., 1990; Gundesø and Egeland, 1990; Omre, 1992; Stanley et al., 1990). This initial work has been further refined by others (Georgsen and Omre, 1993; Hatløy, 1995; Hove et al., 1992; Tjelmeland and More, 1993; Tyler et al., 1992a and b).

FLUVSIM is a convenient public domain fluvial object based algorithm. The algorithm generates stochastic channel streamlines and fits stochastic channel and related architectural element geometries to these streamlines. The FLUVSIM geologic model is based on ribbon sandbodies from typically low net-to-gross systems with primary reservoir quality encountered in sinuous to straight channels and secondary reservoir rock based on levees and crevasse splays embedded in overbank fines (Galloway and Hobday, 1996; Miall, 1996). These ribbon sandbodies are commonly characterized by relatively low width to depth ratios (often <15) and ribbon thickness of less than ten meters (Colinson, 1996). Training images with channel only, channel and levee and channel, levee and splay were calculated (see example training images in Figure 6).

A. Channel Only

Ribbon sandbodies may be highly sinuous to straight. A series of training images were simulated with FLUVSIM to span the scenarios listed in Table 3.

B. Channel and Levee

Significant net facies may be represented in levees (Miall, 1996, p. 172). For the median channel thickness case ribbon sandbodies with levees were simulated. These cases are shown in Table 4. The levee fraction reported in the table is the fraction of the net facies. The levee size is determined by a calibration within the FLUVSIM program.

C. Channel, Levee and Crevasse Splay

Crevasse splay may represent a significant fraction of net facies. For the median channel thickness case ribbon sandbodies with levees fraction the same as channel fraction a variety of scenarios were simulated with crevasse splays. These cases are shown in Table 5. The crevasse splay fraction is the fraction of the net and the remaining net is divided evenly between channel and levee. The levee and crevasse splay size is determined by a calibration within the FLUVSIM program.

Sinuosity is not an input in the current FLUVSIM algorithm. The inputs related to sinuosity are maximum channel deviation from channel axis and the correlation length of the 1D random function that characterizes channel deviation. To characterize the relationship between sinuosity and these parameters the channel generation subroutine was iterated for a variety of deviations and deviation correlation lengths. To remove the ergodic fluctuations the expected term was calculated over ten realizations. There is a clear relationship between sinuosity and the FLUVSIM channel parameters, deviation and deviation correlation length (see Figure 7).

FLUVSIM was modified to more closely reproduce the net-to-gross ratio in the initial object seeding step and the initial temperature in the annealing schedule was set to 0.0, with the maximum iterations set to 20.

Surface Based Training Image

Surface based models are a variation of object based models, although they focus on the object skin or bounding surfaces. These methods, pioneered by Deutsch and others (2001), are amenable to reproducing planar geometries and bed stacking patterns. Pyrcz and Deutsch (2003) developed a surface based algorithm for modeling compensational cycles within turbidite lobes. This model is applied to construct turbidite lobe training images with varying lobe size, net-to-gross fractions and surface irregularity (see Table 6 and see example training images in Figure 8).

The surface correlation controls the regularity of the lobes, with high correlation leading to smooth lobes. The surfaces enclosing the lobes are coded as shale and then the MAPS program is applied to correct the facies proportions to the specific net-to-gross ratio.

Bank Retreat Training Images

The bank retreat model shares the same geometries applied in FLUVSIM with the exception of (1) channel streamlines generated by the disturbed periodic model and fit to cubic splines that allow for high sinuosity features, (2) channel migration and the realistic generation of lateral accretion (point bar) deposits and (3) the formation of abandoned channels and oxbow lakes (see Figure 9). This model is representative of mixed load to suspended load fluvial systems (Galloway and Hobday, p. 400, 1996; Miall, p. 484, 1996). Complete details on the bank retreat model are available in Howard (1992) and Sun and others (1996). Training images with variable net-to-gross fraction, channel width to thickness ratio, initial sinuosity and degree of channel belt amalgamation were calculated (see Table 7 and see example training images in Figure 10).

Correction of Global Category Proportions

Due to ergodic fluctuations and limitations of the algorithms used to calculate the training images, the net-to-gross proportions are not precise in the training images. The global proportions may be corrected to precisely match the representative statistics of the reservoir being modeled by applying the MAPS program.

Selection of the Appropriate Training Image

This library provides a set of training images with a wide variety of fluvial and deepwater features. They may be tailored to represent the geologic features in a broad variety of reservoir settings. The following are some example settings.

Compensation cycles are ubiquitous in distal submarine lobes (Mutti and Sonnino, 1981). These features represent reservoir targets in significant exploration targets in the off shore Gulf of Mexico, West Africa and the North Sea. The surface based training images may be applied represent these compensational features. Post-processing by MAPS may be applied to correct to site specific net-to-gross ratio and the degree of compartmentalization.

Significant resources are available in fluvial reservoirs in areas such as the North Sea (Clemetsen et al., 1990), and East Texas (Galloway and Hobday, 1996). There are a variety of recognized settings. Shoe-string sand bodies in a matrix of overbank and lateral accretion lenses with channel fill mud plugs have been identified in various forms. The FLUVSIM and bank retreat training images may be applied to represent these fluvial settings.

Low to high sinuosity channels and levee complexes have been recognized in deepwater settings. There are some differences between subaqueous and subareal channels. For

example, deepwater channels decrease in width and depth toward the distal due to flow stripping (Flood and Damuth, 1987). Yet, many of the same features are observed (Leeder, 1999). The fluvial training images may be carefully applied to channelized deepwater settings as found in Gulf of Mexico, West Africa and North Sea.

The marked point training images may be applied to a variety depositional settings. This may include bars in coastal settings and lobes in deepwater settings. These training images may be applied directly or may be merged into other training images. For example, bars may be merged into the channel facies of a fluvial training image to represent down stream accretion macroforms (Miall, 1996).

Programs

FORTTRAN programs are included to extract statistics from the training images, perform model operations for the tailoring of training images to specific sites.

Extraction of Multiple-point Statistics from the Training Images

A program called MPSTAT was written to extract multiple-point statistics from the training images. The following statistics may be extracted; (1) multiple-point histograms, (2) transition probabilities, (3) distribution of runs and (4) connectivity functions. Other statistics such as histograms and indicator semivariograms may be calculated with GSLIB programs (Deutsch and Journel, 1998).

Multiple-point statistics are calculated over a specified multiple-point configuration. This configuration is defined by lag vectors, $\mathbf{h}_1, \dots, \mathbf{h}_n$, with $\mathbf{h}_1 = 0$ by convention and is known as a template. The selection of the appropriate template is a function of the available computational resources, and the character and scale of the salient features in the training image (Strebelle, 2002).

A. Multiple Point Histogram

The multiple-point histogram is a multiple-point probability density function (pdf) as defined below and represents the probability of a specific configuration of categories, $1, \dots, K$, existing at the template locations, h_1, \dots, h_N , when the template is scanned over the training image.

$$f(\mathbf{h}_1, \dots, \mathbf{h}_N; k_1, \dots, k_N) = \text{Prob}\{Z(\mathbf{u} + \mathbf{h}_1) \in \text{category } k_1, Z(\mathbf{u} + \mathbf{h}_N) \in \text{category } k_N\} \quad (1)$$

$$k_1, \dots, k_n = 1, \dots, K, \forall \mathbf{u} \in A$$

It is convenient to calculate an index representing as possible configurations of categories, $z(\mathbf{u} + \mathbf{h}_i)$, for template locations, $1, \dots, N$, that may take classes, $1, \dots, K$ (Deutsch, 1992).

$$index = 1 + \sum_{i=1}^N [z(\mathbf{u} + \mathbf{h}_i) - 1] \cdot K^{i-1}, \text{ where } index = 1, \dots, K^N \quad (2)$$

The multiple-point histogram may then be represented as a table of the frequency of each index when the template is scanned over the training image. An example five-point template that may be applied to calculate a multiple-point histogram is shown in the top left of Figure 11.

B. Transition Probability

The transition probability is a subset of the multiple point histogram for the specific case of two points, where the two points are typically adjacent. The transition probability from k_1 to k_2 for lag \mathbf{h} is the probability that given $Z(\mathbf{u})$ is category k_1 that $Z(\mathbf{u} + \mathbf{h})$ is in category k_2 , for $\mathbf{u} \in A$.

$$f(\mathbf{h}; k_1, \dots, k_N) = \text{Prob}(Z(\mathbf{u}) \in \text{category } k_1, Z(\mathbf{u} + \mathbf{h}) \in \text{category } k_N) \quad (3)$$

$$k_1, \dots, k_N = 1, \dots, K, \forall \mathbf{u} \in A$$

This statistic is summarized as a $K \times K$ matrix. This is an intuitive method for visualization of interrelationships of facies. The matrix may not be symmetric due to the lag effect. The transitions for $\mathbf{h} = (0,1)$ are illustrated in the top right of Figure 11.

C. Distribution of Runs

For the categorical case, a run is defined as a sequence of locations with the same category. A single run is parameterized by its length. A specific lag vector, \mathbf{h} identifies the configuration of 1D strings within the training image, $Z(\mathbf{u} + m \cdot \mathbf{h})$ for $\mathbf{u} \in A$ and m is any integer such that $\mathbf{u} + m \cdot \mathbf{h} \in A$. All possible strings are extracted and the distribution of runs is calculated. The associated probability may be shown as:

$$\text{Prob}\{\text{Run of Length } M\} = \text{Prob}\{Z(\mathbf{u}) \in \text{category } k_i, Z(\mathbf{u} + \mathbf{h}) \in \text{category } k_i, \dots, Z(\mathbf{u} + M\mathbf{h}) \in \text{category } k_i, Z(\mathbf{u} + (M+1)\mathbf{h}) \notin \text{category } k_i\} \quad (4)$$

$$k_i = 1, \dots, K, \forall \mathbf{u} \in A$$

The statistic is summarized as table with the length of run and associated frequency. The distribution of runs is illustrated for $\mathbf{h} = (0,1)$ in the bottom right of Figure 11.

D. Connectivity Function

The connectivity function calculates geo-objects for the identified net categories. The output is the original training image categories and the associated geo-object index, set as

null for non-net categories. A fast algorithm is applied and the user specifies whether edges and corners allow for communication (Deutsch, 1998b).

The parameter file associated with the MPSTATS program is shown in Figure 12 and a summary of the input parameters is included below.

- *Line 1* – input file. The file should be in GEOEAS format.
- *Line 2* – column number with the associated categorical data.
- *Line 3* – trimming limits. Data outside of these limits are omitted from the calculations.
- *Line 4* – size of the input model. See Figure 1.
- *Line 5* – number of facies and the associated indices.
- *Line 6* – the number of pay facies and the associated indices. This is only used for the calculation of the connectivity function.
- *Line 7* – the type of calculation:
 - Option #1 - multiple point histogram
 - Option #2 - transition probabilities
 - Option #3 - connectivity function and
 - Option #4 - distribution of runs
- *Line 8* – the number of cells in the template (option 1) or the lags (option 2 and 4). Note for multiple point histograms the location 0 is assumed at 0,0,0; therefore, a template with 4 cells defines a 5 point histogram. For transition probabilities and distribution of runs results are calculated for each lag separately.
- *Line 9 to 12* – the relative locations of the template nodes / lags. These are integers representing number of cells relative to location 0.
- *Line 13* – logical switches for accounting for edge and corner connections. This is only used for the calculation of the connectivity function.
- *Line 14* – the output file.

Multiple-point histogram output is in GEOEAS format, with K^N rows, and columns with the indices (see Equation 2), the categories at locations $\mathbf{h}_1, \dots, \mathbf{h}_N$, the frequency and the conditional probability of category $z(\mathbf{h}_1)$ given $z(\mathbf{h}_2), \dots, z(\mathbf{h}_N)$. These conditional probabilities may be read directly into a multiple point simulation algorithm.

The transition probabilities output is a $K \times K$ matrix with the probability of transition. This output may be applied directly to infer quantitative interrelationships as required by truncated Gaussian methods.

The output for the connectivity function is the original training image with the connected object index number appended in GEOEAS format. This index may be applied to visualize and quantify connected geo-objects. This information may be applied to assess recovery factors and morphologies for object based simulation.

The distribution of runs output is GEOEAS, with N rows (where N is the maximum run length), and columns with the length of run and the frequency. This output may be

applied as soft information on connectivity or as input to simulation algorithms that consider the distribution of runs (Ortiz, 2003).

Model Operations

A program called MODELOPS is provided to tailor the training images to a specific site. This program performs operations such as: (1) arithmetic operations on multiple models, (2) merging two models, (3) extracting subsets and (4) grouping facies. The program reads in multiple models from any number of files and then performs model operations sequentially. The output may represent the entire model or a subset of the model (see an example parameter file in

Figure 13).

- *Line 1* – the number of input data files, number of operations to perform and the trimming limits. If any data is trimmed then that model location is set as null for all output.
- *Line 2 to 5* – the input data files, the number of data from each file and the associated columns. The input data are indexed in logical order, for example is there are two data files each with two data then: $data_1$ and $data_2$ are the first and second data from the first file and $data_3$ and $data_4$ are the first and second data from the second file.
- *Line 6* – the size of the input models
- *Line 7 and 8* – the list of operations, the format generally follows this format, $data_1^i \text{ operation}^i data_2^i \text{ equals } data_3^i$.
 - *Operation #1*: addition ($d_1+d_2=d_3$)
 - *Operation #2*: subtraction ($d_1-d_2=d_3$)
 - *Operation #3*: multiplication ($d_1 \times d_2=d_3$)
 - *Operation #4*: division ($d_1/d_2=d_3$)
 - *Operation #5*: exponent ($d_1^{d_2}=d_3$)
 - *Operation #6*: merge two categories (d_2 set to d_1 if $d_2 = d_3$)
 - *Operation #7*: group (set cat_1 and cat_2 as cat_1 in d_3) Note: for this operation the command is: $cat_1 \ cat_2 \ op \ d_3$.
- *Line 9* – the output file.
- *Line 10* – the number of data to write out and a list of their indices
- *Line 11 to 13* – the output model size. In this example the original model is written out. This allows subsets to be written out.

MODELOPS is illustrated for an example with two data files, with two data from the first file and one from the second. The first selected column from file #1 is $data_1$, the second selected column is $data_2$ and the selected column from the second file is $data_3$. The following example operations are performed:

- 2 1 7 3 - Operation#1: $cat_1, cat_2, op, data_1$
- 1 2 1 4 - Operation#2: $data_1, data_2, op, data_3$
- 3 4 3 5 - Operation#3: $data_1, data_2, op, data_3$

Categories 1 and 2 are grouped as category 2 in data₃. Data₁ and data₂ are added together and become data₄. Product of data₃ and data₄ become data₅. Any combination of data₁ through data₅ may be included in output file.

Reformatting

Coordinates may be added with the ADDCOORD program from GSLIB (Deutsch and Journel, 1998). The ADDCOORD source may be modified to adjust the format and order for input to a variety of software packages.

Anticipated Applications

There is a wide variety of anticipated applications for the fluvial and deepwater training image library. (1) Primarily, these training images may be applied to aid in the inference to input statistics for conventional semivariogram and multiple-point based geostatistical models. (2) They may be utilized in comparative flow studies, for the calculation of recovery factors for reserves, to assess connectivity and to quantify geo-objects for input into object based simulation methods. (3) This library provides a documented set of “type-models” that demonstrate the capabilities and limits of geostatistical models and may be applied to help newcomers understand the techniques, tools and algorithms available in geostatistics. (4) This library provides scenarios for uncertainty analysis that is especially useful in frontier reservoirs.

Inference of Input Statistics

The primary application of these training images is to aid in the inference of input statistics for conventional semivariogram based and multiple-point geostatistical models. Training images may be chosen from the existing library or tailored by merging a variety of training images, such that spatial features deemed relevant to the site being characterized are represented.

The indicator semivariogram model is an important input for pixel based categorical geostatistical algorithms such as sequential indicator and truncated Gaussian simulation. The inference of the indicator semivariogram model is often problematic because of sparse data. Analysis of the experimental indicator semivariograms from the appropriate training images may provide information on the nested structures, associated shapes and range of correlation, in the principal directions. This information combined with the available experimental indicator semivariograms will result in improved indicator semivariogram model inference.

The need for training images in multiple-point geostatistical algorithms has been discussed. This training library provides a wide variety of high resolution training images and the tools to tailor them to a specific site and to extract the required consistent multiple-point statistics. This library makes the application of multiple-point geostatistics more practical.

Comparative Flow Studies

In practice only a small fraction of reservoirs are subjected to full flow simulation studies. In the absence of full flow simulation, these training images may be applied to aid in the inference of recovery factors and to quantify the connectivity, geometries and features that may constrain reservoir response.

Recovery factors may represent an important parameter in the exploratory stage of reservoir development. The training images may be applied to calculate the potential recovery factors given the recovery method and expected geologic features. The resulting distribution of recovery factors may be applied to aid in reservoir management decisions.

Connectivity and geometry may significantly constrain reservoir response. The training images provide various models that contain characteristic fluvial and deepwater features that may be analyzed for the formation of barriers, baffles and conduits. Connected geo-objects may be calculated to assess the potential for compartmentalization. In addition, the identified geo-objects may be quantified and integrated into an object based simulation algorithm.

Documented “Type Models”

These training images represent documented type models that demonstrate features that geostatistical models are able to reproduce and their associated limits. The features reproduced in these training images, may be compared and contrasted with other spatial models, such as fractals, neural nets and other pattern recognition techniques and genetic algorithms and may aid in the integration of secondary data such as seismic and production data. Also, these type models may be applied as training tools.

All models have unique underlying assumptions that may significantly affect the simulated distribution of response variables after a transfer function. For example, the multi-Gaussian (MG) distribution assumption results in maximum disorder of the extremes. Models based on the MG distribution may result in exaggerated dispersive flow and may under represent the presence of conduits, barriers and baffles to flow. The training image models may be compared with models generated by other algorithms to assess the impact of model assumptions after the application of a transfer function.

Production data from well tests provide large scale information such as the permeability near the well and may aide in predicting the insitu resource and the limits of the reservoir. Seismic provides large scale structural information. This large scale data may be integrated into the reservoir model by choosing a training image based on its match with production and seismic data. For example, production data and seismic information may indicate unconnected channelized sandbodies and this information may be applied to choose appropriate training images.

These training images represent a variety of object and surface based geostatistical algorithms. These training images demonstrate a wide variety of input statistics and parameters that may be reproduced by geostatistical algorithms; therefore, they may be applied as a training tool for geologists, engineers, geophysicists and other professionals that are involved in reservoir characterization. Some of these algorithms reproduce complicated geometries and interrelationships; this may inspire additional research into the integration of geologic information into geostatistical models.

Library for Scenario Based Uncertainty Study

There is often a high degree of uncertainty with respect to reservoir morphologies; with respect to the present geometries (e.g. lobes or channels), and their associated properties (large or small lobes or channels). This uncertainty may be quantified through the assignment of scenarios with their associated probabilities based on the available data, analogue information and expert judgment. The uncertainty in reservoir morphologies may be modeled by calculating multiple realizations with training images drawn from the identified scenarios (Pyrcz et. al, 2003).

An example scenario tree is shown in Figure 14. For this example there is uncertainty with respect to the depositional setting, architectural elements and the scale of the sandbodies. Conditional probabilities are assigned for each decision and the probability of each scenario is calculated. Recall:

$$\text{Prob}(A, B, C) = \text{Prob}(C | A, B) \cdot \text{Prob}(B | A) \cdot \text{Prob}(A) \quad (5)$$

Training images may be selected that meet these criteria. Then realizations based on a multiple point stochastic algorithm may be calculated with training images drawn from the selected scenarios.

Summary

The training image library includes object and surface based geostatistical algorithms for fluvial and deepwater settings. The training images represent a variety of features. Some depositional settings such as eolian and coastal are not directly represented. Future work will address more clastic depositional settings and morphologies.

The training images represent a variety of model parameters such as net-to-gross ratio, sinuosity, channel width and width to depth ratio and lobe size. Storage constraints limited the number of scenarios considered and the number of parameters varied.

The associated code aids the practitioner to tailor to the training images to a specific site and to calculate, extract and format multiple-point statistics. Multiple models may be modified by arithmetic operations, merged by category to represent a hierarchy of heterogeneity and categories may be grouped. There is no provision in the associated code for complicated operations such as operations on subsets, rotation and scaling. Future work may address more complicated model operations.

Multiple-point statistics may be extracted from the training images. The large size of the models should result in interpretable statistics. The calculation of statistics on these training images requires significant computational effort. The training images may be down scaled or trimmed to smaller subsets to reduce computational effort.

References

Clemensten, R., Hurst, A.R., Knarud, R., Omre, H., 1990. A computer program for evaluation of fluvial reservoirs. In: Buller, A.T., Berg, E., Hjelmeland, O., Kleppe, J., Torsæter, O, Aasen, J.O., (Eds.), North Sea Oil and Gas Reservoirs II. Graham and Trotman, London, pp. 372–385.

Collinson, J.D., Alluvial sediments. In: Reading, H.G. (Eds.), Sedimentary Environments: Processes, Facies and Stratigraphy. Blackwell Science, Oxford, pp. 37-82.

Deutsch, C.V., 1992, Annealing Techniques Applied to Reservoir Modeling and the Integration of Geological and Engineering (Well Test) Data, Ph.D. Thesis, Stanford University (306 pp.).

Deutsch, C.V., 1998a, Cleaning categorical variable (lithofacies) realizations with maximum a-posteriori selection. *Computers & Geosciences*, 24 (6), 551-562.

Deutsch, C.V., 1998b, FORTRAN programs for calculating connectivity of 3-D numerical models and for ranking multiple realizations. *Computers & Geosciences*, 24 (1), 69-76.

Deutsch, C.V. and Journel, A.G., 1998, GSLIB: Geostatistical Software Library and Users Guide, 2nd ed. Oxford University Press, New York (369 pp.).

Deutsch, C.V. and Wang, L., Hierarchical object-based stochastic modeling of fluvial reservoirs. *Math Geology*, 28 (7), 857-880.

Deutsch, C.V. and Tran, T.T., 2002, FLUVSIM: a program for object-based stochastic modeling of fluvial depositional systems. *Computers and Geosciences*, 28 (2002) 525-535.

Deutsch, C.V., Xie, Y., and Cullick, A.S., 2001, Surface geometry and trend modeling for integration of stratigraphic data in reservoir models, Proceedings 2001 SPE Western Regional Meeting. Bakersfield, California.

Flood, R.D. and Damuth, J.E., 1987, Quantitative characteristics of sinuous distributary channels on the Amazon deep-sea fan. *Geologic Society of America Bulletin*, 98, 728-738.

Galloway W.E. and Hobday, D.K., 1996, Terrigenous Clastic Depositional Systems: Springer, New York (489 pp.).

Georgsen, F. and Omre, H., 1993. Combining fibre processes and Gaussian random functions for modeling fluvial reservoirs. In: Soares, A., (Eds.), *Geostatistics Troia 1992*, Vol. 2, Kluwer, Dordrecht, pp. 425–440.

Gundesø, R., Egeland, O., 1990. SESIMIRA—a new geologic tool for 3-d modeling of heterogeneous reservoirs. In: Buller, A.T., Berg, E., Hjelmeland, O., Kleppe, J., Torsæter, O., Aasen, J.O., (Eds.), *North Sea Oil and Gas Reservoirs II*. Graham and Trotman, London, pp. 360–371.

Hatloy, A.S., 1995. Numerical facies modeling combining deterministic and stochastic method. In: Yarus, J.M., Chambers, R.L. (Eds.), *Stochastic Modeling and Geostatistics: Principles, Methods, and Case Studies*, AAPG Computer Applications in Geology, pp. 109–120.

Hove, K., Olsen, G., Nilsson, S., Tonnesen, M., Hatloy, A., 1992. From stochastic geological description to production forecasting in heterogeneous layered reservoirs. SPE Annual Conference and Exhibition, Washington, DC, SPE Paper Number 24890, 311–325.

Howard, A.D., 1992, Modeling channel migration and floodplain sedimentation in meandering stream. In: Carling, P.A., Petts, G.E., (Eds.), *Lowland Floodplain Rivers: Geomorphological Perspectives*. John Wiley and Sons, New York, pp. 1-37.

Journel, A. and Alabert, F., 1989, Non-Gaussian data expansion in the earth sciences. *Terra Nova*, 1, 123-134.

Leeder, M.R., 1999, *Sedimentology and Sedimentary Basins; from Turbulence to Tectonics*, Balckwell, Oxford (592 pp.).

Miall, A.D., 1996, *The Geology of Fluvial Deposits: Sedimentary Facies, Basin Analysis and Petroleum Geology*. Springer-Verlag Inc., Berlin (582 pp.).

Omre, H., 1992. Heterogeneity models. In *SPOR Monograph: Recent Advances in Improved Oil Recovery Methods for North Sea Sandstone Reservoirs*, Norway. Norwegian Petroleum Directorate, pp. 141–153.

Ortiz, J., 2003, *Characterization of High Order Correlation for Enhanced Indicator Simulation*, Ph.D. Thesis, University of Alberta, (243 pp.).

Pyrcz, M.J. and C. V. Deutsch, 2003, Stochastic surface modeling in mud rich, fine-grained turbidite lobes, AAPG Annual Meeting, Salt Lake, Utah.

Pyrcz, M.J. and Deutsch, C.V., 2003, Bank retreat meandering fluvial process based model. Centre for Computational Geostatistics 5th Annual Report, University of Alberta.

Pyrcz, M.J., Gringarten, E., Frykman, P., and Deutsch, C.V., 2003, Representative input parameters for geostatistical simulation. In: Coburn, T.C., (Eds.), *Stochastic Modeling II. AAPG Computer Applications in Geology*, No. N.

Stanley, K.O., Jorde, K., Raestad, N., Stockbridge, C.P., 1990. Stochastic modeling of reservoir sand bodies for input to reservoir simulation, Snorre Field, northern North Sea. In: Buller, A.T., Berg, E., Hjelmeland, O., Kleppe, J., Torsæter, O, Aasen, J.O., (Eds.), *North Sea Oil and Gas Reservoirs II*. Graham and Trotman, London, pp. 91–103.

Stoyan, D., Kendall, W.S., Mecke, J., 1987, *Stochastic Geometry and Its Applications*. John Wiley & Sons, New York (345 pp.).

Strebelle, S., 2002, Conditional simulation of complex geological structures using multiple-point statistics. *Math Geology*, 34 (1), 1-22.

Sun, T., Meakin, P. and Jossang, T., 1996, A simulation model for meandering rivers. *Water Resources Research*, 32 (9), 2937-2954.

Tjelmeland, H. and Omre, H., 1993. Semi-Markov random fields. In: Soares, A., Editor, , 1993. *Geostatistics Troia 1992*, Vol. 2, Kluwer, Dordrecht, pp. 493–504.

Tyler, K., Henriquez, A., Georgsen, F., Holden, L., Tjelmeland, H., 1992a. A program for 3d modeling of heterogeneities in a fluvial reservoir. *Proceedings 3rd European Conference on the Mathematics of Oil Recovery*, Delft, June, pp. 31–40.

Tyler, K., Henriquez, A., MacDonald, A., Svanes, T., Hektoen, A.L., 1992b. MOHERES—a collection of stochastic models for describing heterogeneities in clastic reservoirs. *Proceedings 3rd International Conference on North Sea Oil and Gas Reservoirs III*, pp. 213–221.

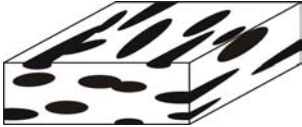
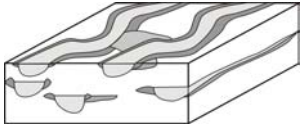
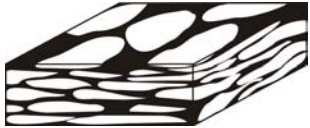
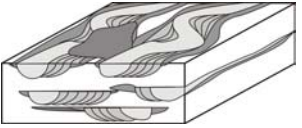
Model Type	Number of Models	Categories	Schematic
Marked Point			
Lobe	12	Object Matrix	
Ellipse	12		
Bar	12		
FLUVSIM			
Channel	108	Channel Levee Splay Overbank Fines	
Channel and Levee	108		
Channel, Levee and Splay	108		
Surface Based			
Compensational cycles of lobes	36	Lobe Shale	
Bank Retreat			
Channel complex	108	Abandoned Channel Point Bar Levee Crevasse Splay Overbank Fines	

Table 1 – summary table of the training image library with schematic representations of the models.

NTG	Scale (m)	Geometry
0.2	500	Ellipse
0.4	1000	Lobe
0.6	1500	Bar
0.8		

Table 2 – the parameters for the marked point process scenarios.

NTG	Channel Thickness (m)	Width:Thickness	Sinuosity
0.2	2	20	1.0
0.4	4	50	1.5
0.6	7	100	2.0
0.8			

Table 3 – scenarios for the channel only ribbon sandbody training images.

NTG	Channel Thickness (m)	Width:Thickness	Sinuosity	Levee Fraction
0.2	4	20	1.0	0.2
0.4		50	1.5	0.5
0.6		100	2.0	0.8
0.8				

Table 4 – scenarios for the channel with levee ribbon sandbody training images.

NTG	Channel Thickness (m)	Width:Thickness	Sinuosity	Levee Fraction	Crevasse Splay Fraction
0.2	4	20	1.0	same as channel	0.2
0.4		50	1.5		0.5
0.6		100	2.0		0.8
0.8					

Table 5 – scenarios for the channel with levee and crevasse splay ribbon sandbody training images.

NTG	Surface Correlation	Lobe Size
0.2	Low	Small
0.4	Median	Median
0.6	High	Large
0.8		

Table 6 - scenarios for the surface based turbidite lobe training images.

NTG	Channel Thickness (m)	Width:Thickness	Sinuosity	Amalgamation
0.2	4	10	1.0	Low
0.4		30	1.5	Medium
0.6		100	2.0	High
0.8				

Table 7 - scenarios for the bank retreat training images.

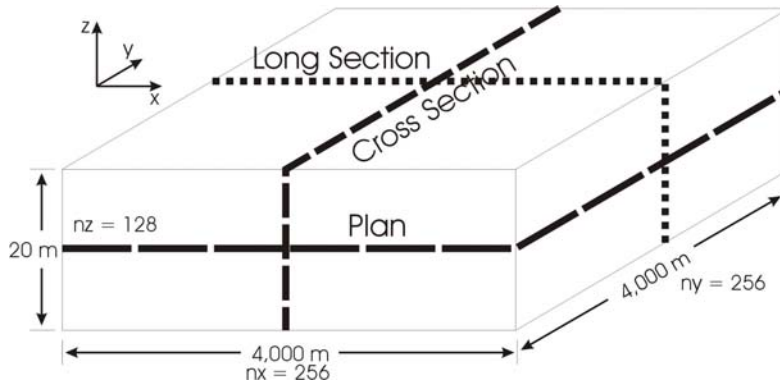


Figure 1 – the nominal model size, the level of discretization and the model origin. The plan, long and cross sections used in subsequent visualizations are indicated.

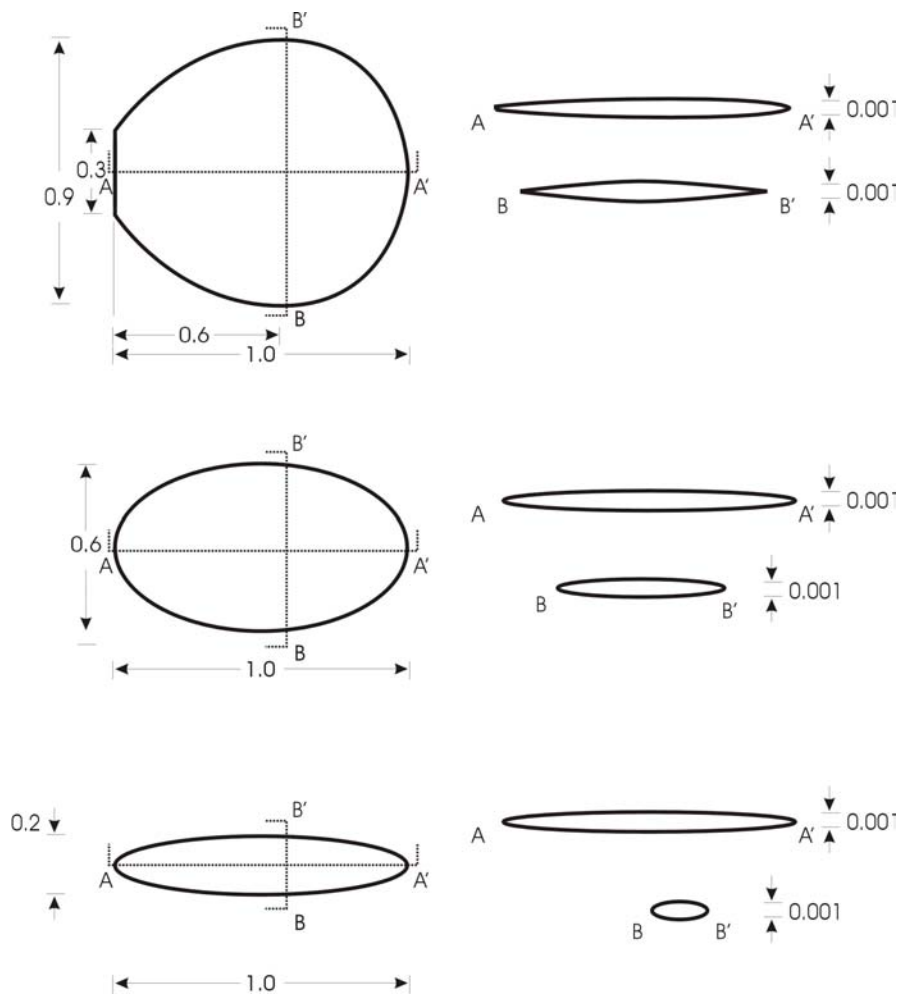


Figure 2 – the templates for the marked point processes (Lobe – Top, Ellipsoid – Middle and Bar – Bottom). The units are in the fraction of the randomly assigned scale (see Table 2). Schematic is not to scale.

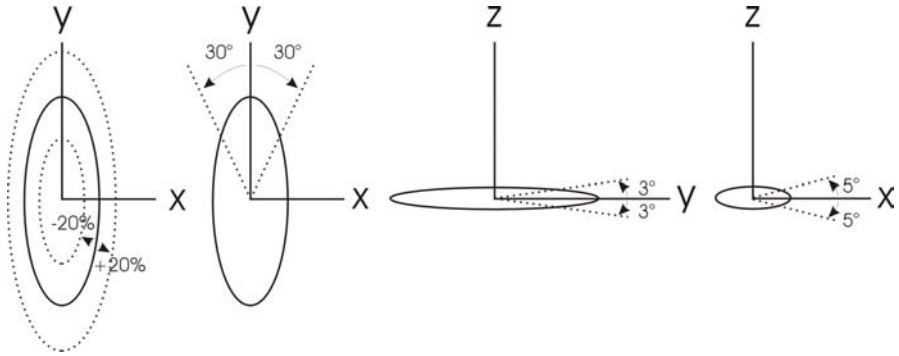


Figure 3 – a schematic of the stochastic transforms applied to the primary grain. From left to right they are scale, azimuth, dip and plunge.

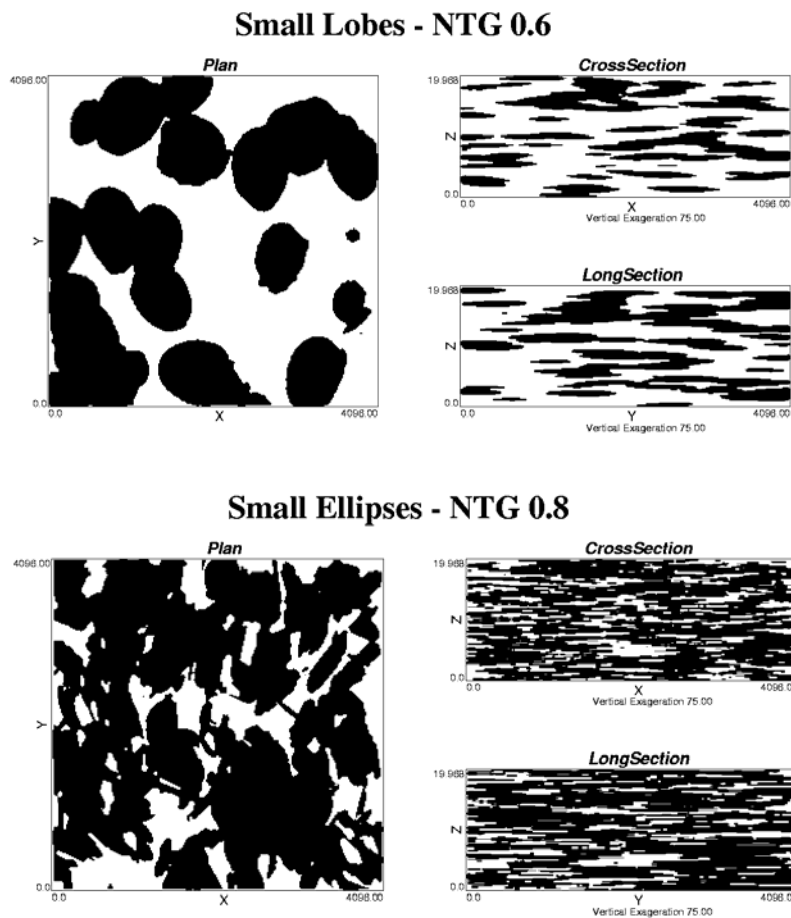


Figure 4 – example marked point process training images. Plan view, cross section and long section slices taken from the center of training image.

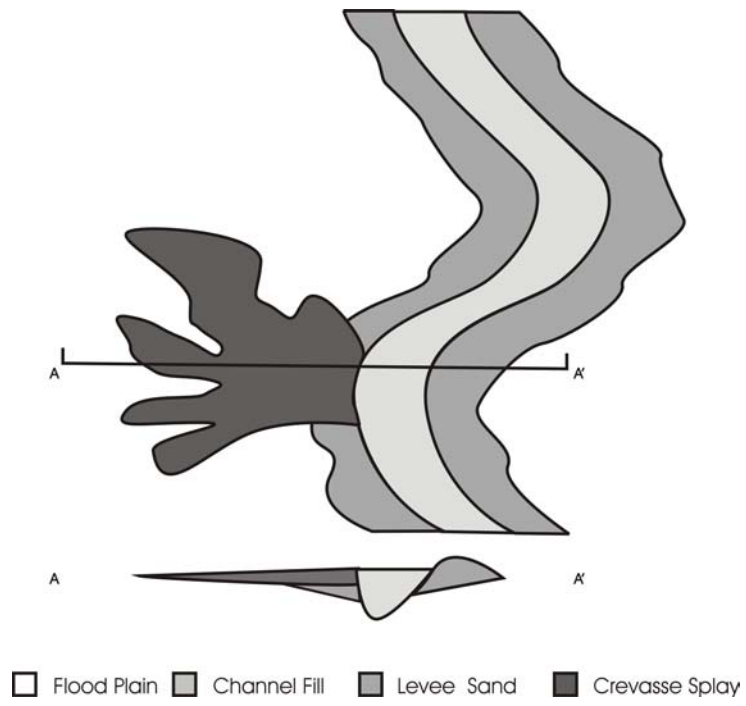
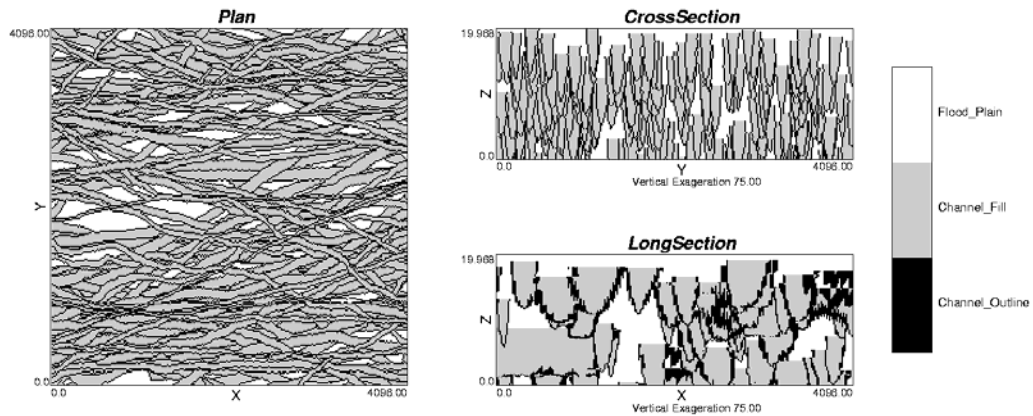
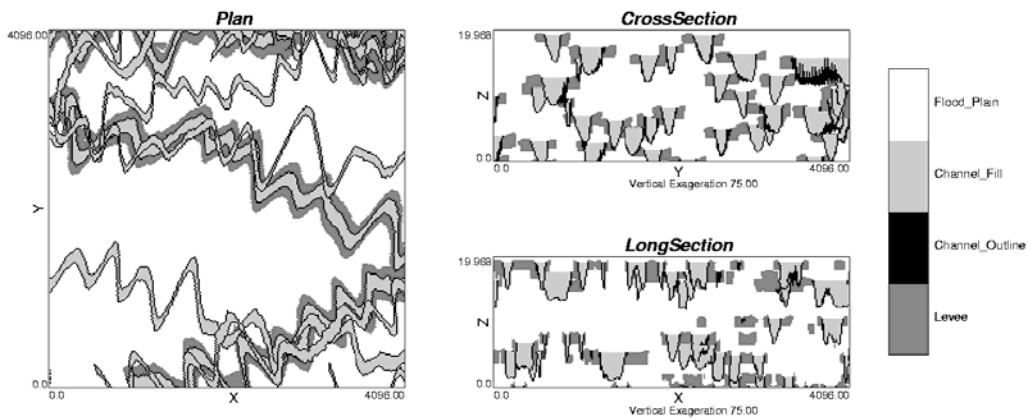


Figure 5 – the FLUVSIM model.

Channel Only - W:T 20 - Low Sinuosity - NTG 0.8



Channel and Levee - W:T 50- High Sinuosity - NTG 0.4



Channel, Levee, and Splay - W:T 100 - Median Sinuosity - NTG 0.2

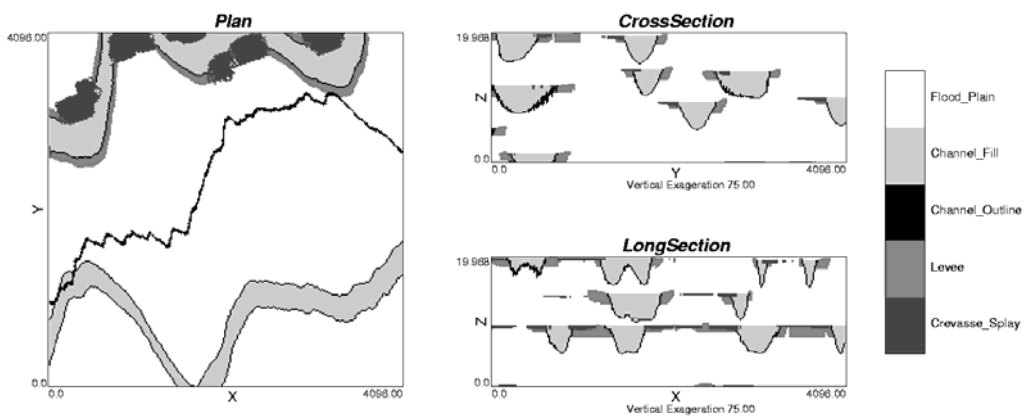


Figure 6 - example FLUVSIM training images. Plan view, cross section and long section slices taken from the center of training image.

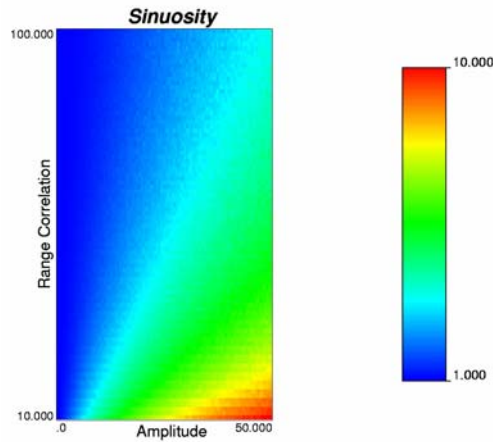
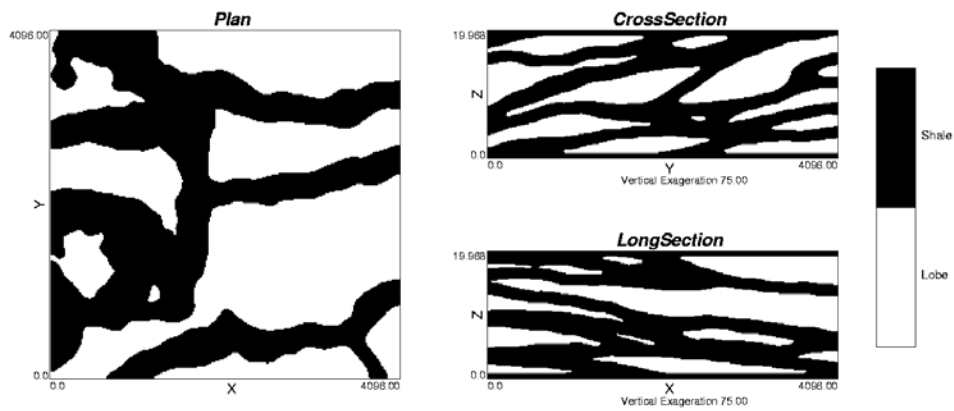


Figure 7 – the relationship between deviation, deviation correlation length and sinuosity.

Large Lobes - Low Correlation - NTG 0.4



Small Lobes - High Correlation - NTG 0.8

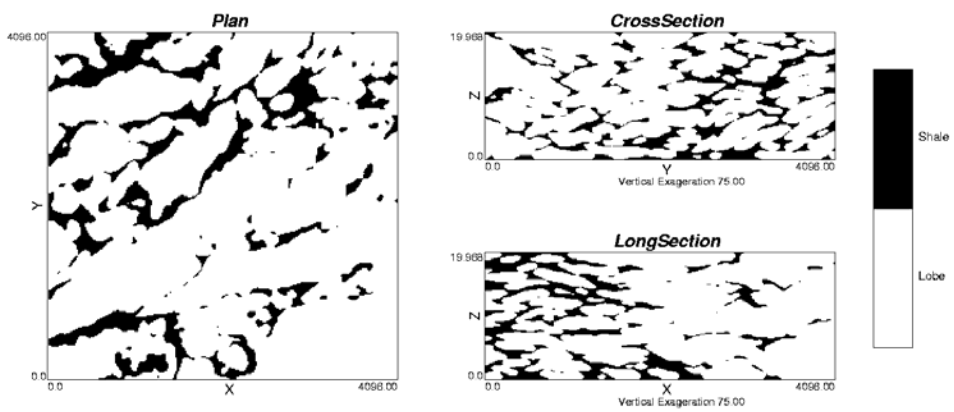


Figure 8 - example surface based training images. Plan view, cross section and long section slices taken from the center of training image.

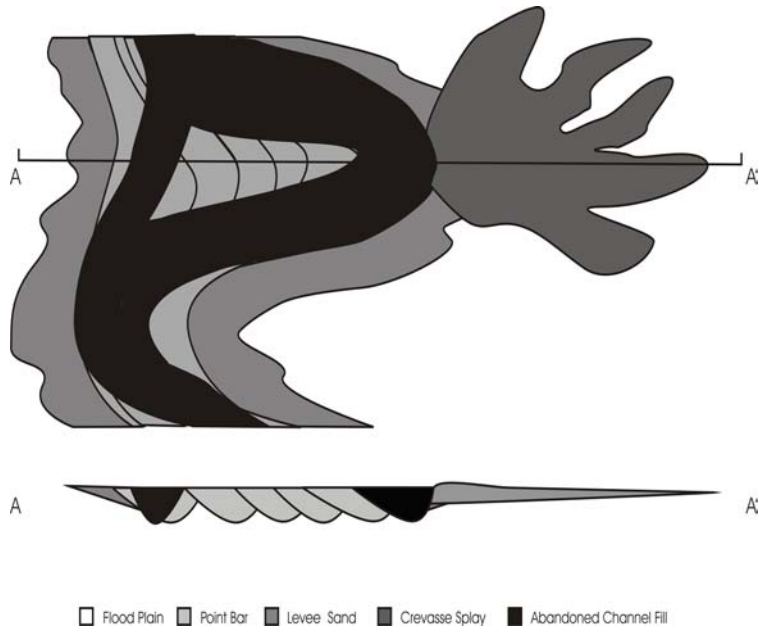
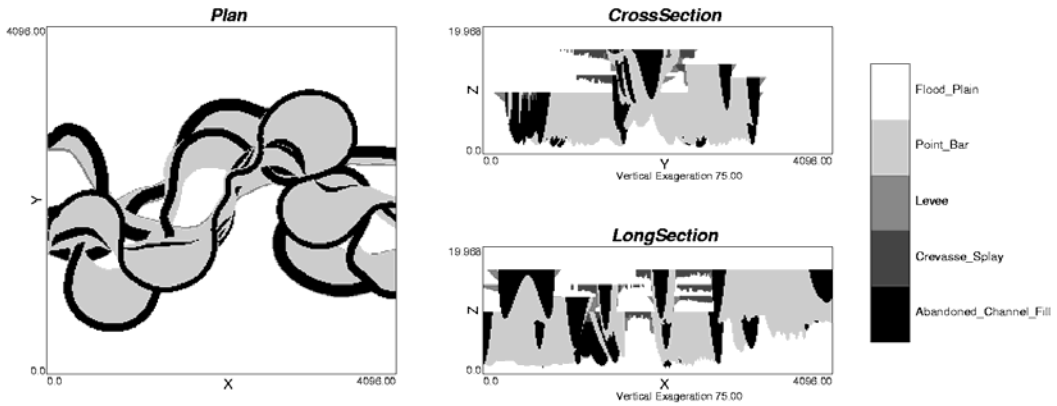


Figure 9 – the bank retreat fluvial model.

High Amalgamation - W:T 20 - Median Sinuosity - NTG 0.2



Low Amalgamation - W:T 20 - High Sinuosity - NTG 0.4

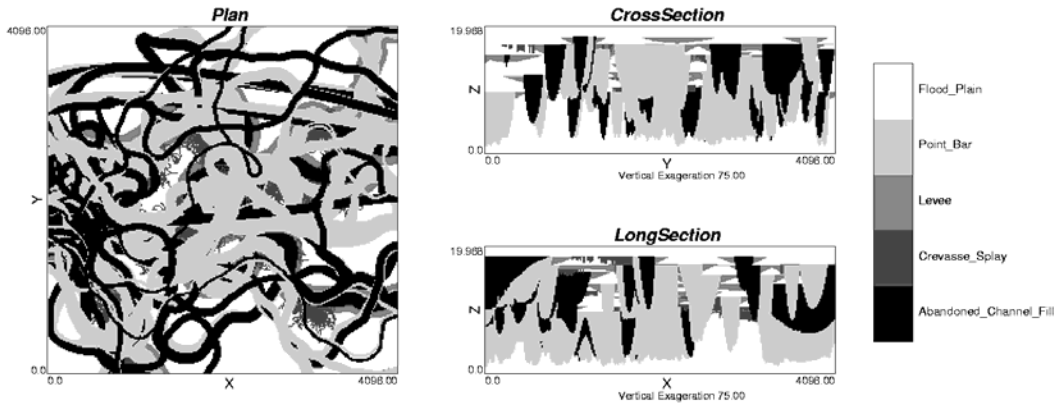


Figure 10 - example bank retreat training images. Plan view, cross section and long section slices taken from the center of training image.

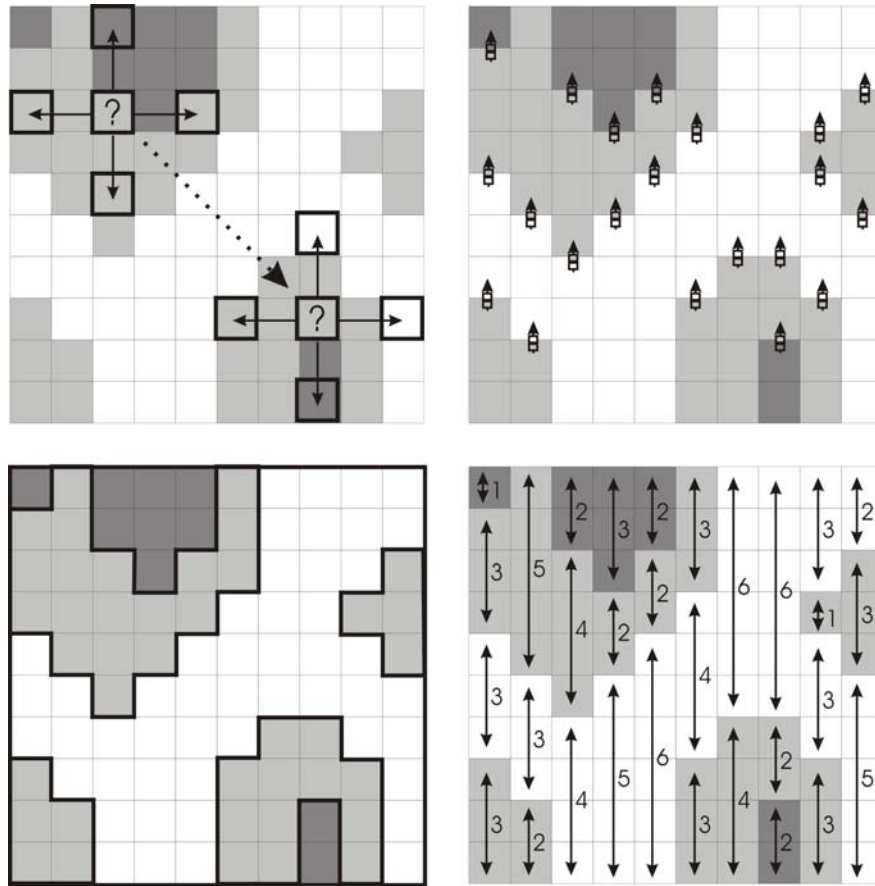


Figure 11 – schematic representation of the multiple point statistics calculated with the *mpstats* program. Top Left – multipoint histograms, a template is scanned through the image and the frequency of specific configurations is stored, Top Right – transition probabilities are the probability of contact between two facies, note the intervals without transition are also considered, but are not shown in the schematic to avoid clutter, Bottom Left – connectivity functions, the image is divided into connected geo-objects, Bottom Right – the distribution of runs.

Parameters for MPSTATS		

<i>Line 1</i>	model.dat	-file with model
<i>Line 2</i>	1	-column
<i>Line 3</i>	0.0 100.0	-tmin, tmax
<i>Line 4</i>	256 256 128	-nx,ny,nz
<i>Line 5</i>	3 1 2 3	-number of facies, facies:1,...,nfacies
<i>Line 6</i>	1 2	-number of pay facies, pay: 1,...,npay (option 3 only)
<i>Line 7</i>	1	-option (1-np hist., 2-trans. prob., 3-conn. func., 4-runs)
<i>Line 8</i>	4	-number of cells in template (option 1)/ lags (option 2 and 4)
<i>Line 9</i>	-1 -1 0	-cell #1 in template / lag #1: x,y,z relative
<i>Line 10</i>	0 1 0	-cell #2 in template / lag #2: x,y,z relative
<i>Line 11</i>	1 0 0	-cell #3 in template / lag #3: x,y,z relative
<i>Line 12</i>	1 -1 0	-cell #4 in template / lag #4: x,y,z relative
<i>Line 13</i>	1 1	-testedge, testcorner (option 3 only)
<i>Line 14</i>	mpstats.out	-output file

Figure 12 - the MPSTATS parameter file.

Parameters for MODELOPS		

<i>Line 1</i>	2 2 -1.0 100.0	-nfile, nop, tmin, tmax
<i>Line 2</i>	data1.dat	-datafl#1
<i>Line 3</i>	1 1	-datafl#1: ndata, cols
<i>Line 4</i>	data2.dat	-datafl #2
<i>Line 5</i>	1 1	-datafl#1: ndata, cols
<i>Line 6</i>	256 256 128	-nx,ny,nz
<i>Line 7</i>	1 2 1 3	-operation#1: d1, d2, op, d3
<i>Line 8</i>	1 3 1 4	-operation#2: d1, d2, op, d3
<i>Line 9</i>	modelops.out	-output file
<i>Line 10</i>	4 1 2 3 4	-nout, values
<i>Line 11</i>	1 256	-osx,osx
<i>Line 12</i>	1 256	-osy,osy
<i>Line 13</i>	1 128	-osz,oez

Figure 13 - the MODELOPS parameter file.

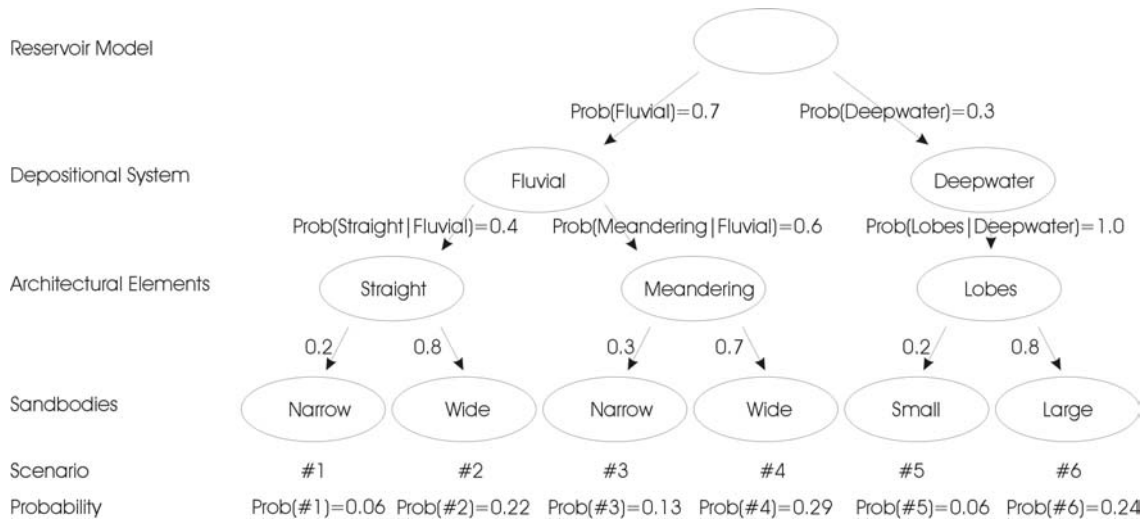


Figure 14 – a potential scenario tree for a reservoir model with uncertainty with respect to the depositional system, architectural elements and sandbody geometry. The resulting probabilities for each scenario may be applied for drawing training images.